Fluorescent Proteins as Proteomic Probes*[S]

Ileana M. Cristea‡, Rosemary Williams§, Brian T. Chait‡¶, and Michael P. Rout§‖

Protein complexes mediate the majority of cellular processes. Knowledge of the localization and composition of such complexes provides key insights into their functions. Although green fluorescent protein (GFP) has been widely applied for *in vivo* visualization of proteins, it has been relatively little used as a tool for the isolation of protein complexes. Here we describe the use of the standard GFP tag to both visualize proteins in living cells and capture their interactions via a simple immunoaffinity purification procedure. We applied this method to the analysis of a variety of endogenous protein complexes from different eukaryotic cells. We show that efficient isolations can be achieved in 5–60 min. This rapid purification helps preserve protein complexes close to their original state in the cell and minimizes nonspecific interactions. Given the wide use and availability of GFP-tagged protein reagents, the present method should greatly facilitate the elucidation of many cellular processes. ***Molecular & Cellular Proteomics 4:1933–1941, 2005.***

Protein complexes mediate the majority of cellular processes. Localization of such complexes provides key insights into their functions. There are a variety of tools for localizing individual proteins in space and time in the cellular milieu (1). Among the most widely used is the green fluorescent protein (GFP)[1] (1, 2), which provides a convenient *in vivo* tag for following the dynamics of gene expression and protein localization (3). For example, GFP was recently used to genomically tag more than 4000 proteins for a large scale analysis of protein localization in *Saccharomyces cerevisiae* (4).

As well as localization, information on the composition of protein complexes provides key functional insights. Thus, a variety of methods have been devised for the study of protein interactions (5). Of these, immunoaffinity purification provides an effective means for isolating protein complexes and elucidating their composition (6). Immunoisolation is achieved with antibodies directed either 1) specifically against the proteins of interest or 2) against tags that are coupled to the proteins of interest. In the first of these strategies, production of high quality antibodies for each protein of interest can be time-consuming and expensive. Moreover the efficacy of this approach depends strongly on the specificity and affinity of the antibody, which in turn may depend on the antigenicity of the protein in question. The second strategy, utilizing tagged proteins, is attractive because a single highly optimized antibody can serve as the immunoaffinity reagent. Commonly used tags include the FLAG and MYC peptides and Protein A (7). Recently the use of multiple tags, such as the two-step tandem affinity purification tag strategy, has become popular (8). Although all these tags have proved highly effective for the isolation of protein complexes, they cannot be readily visualized in living cells. Although GFP has the potential to serve as both a visualization and isolation tag, it has only occasionally been used for immunoaffinity purifications (9–15, 49). One highly attractive option would be a simple, rapid procedure that can be applied to any GFP-tagged construct. Here we describe how the use of GFP to both visualize proteins in live cells and capture their interactions via immunoaffinity purification on magnetic beads promises to facilitate our understanding of the temporal and spatial dynamics of protein interactions.

MATERIALS AND METHODS

GFP Reagents—GFP was in-house cloned into the pGex 4T-3 vector, which contains the GST open reading frame, expressed from an inducible tac promoter, and immediately upstream of a thrombin cleavage site (Invitrogen). The GFP open reading frame was inserted in-frame between the SalI and NotI restriction enzyme sites in the multiple cloning sequence of this vector to create a single GST-thrombin cleavage site-GFP open reading frame. The resulting expression vector was freshly transformed into BL21 cells before each preparation. Two-liter cultures were grown at 37 °C in LB medium (Fisher) with ampicillin until A_{600} reached ~0.5. Cultures were then transferred to 30 °C and induced with 0.5 mM isopropyl β-D-thiogalactoside (Stratagene) for 3.5 h. Cells were harvested, and pellets were resuspended in lysis buffer (PBS, 2 mM EDTA, 1:200 protease inhibitors (16) to make up to a total of 200 ml). Cells were lysed using an M110S microfluidizer (Microfluidics International Corp., Newton, MA). Alternatively lysis could be performed by French press or other methods. Cell debris were removed by centrifugation in an SS-34 swinging bucket rotor (Sorvall centrifuge RC-5B) at 10,000 rpm for 30 min at 4 °C. A glutathione-Sepharose column was prepared for the purification of the GST-GFP fusion protein. Glutathione-Sepharose (2.5-ml bed volume) was added to a small column using a peristaltic pump and washed with 200 ml of lysis buffer. Sample was loaded onto the resin with two discrete passes through the column at 5 ml/min flow rate. The resin was washed with 250 ml of lysis buffer with protease inhibitors and 250 ml without protease inhibitors and allowed to drip to almost dry. The column was sealed, and 10 ml of lysis buffer, 1 mM DTT, and 100 units of thrombin (Amersham Biosciences) were added. The sample was cleaved from the resin by an overnight incubation at 4 °C with gentle rotation after which the eluted protein was drained

From the ‡Laboratory for Mass Spectrometry and Gaseous Ion Chemistry and the §Laboratory of Cellular and Structural Biology, The Rockefeller University, New York, New York 10021

Received, July 21, 2005, and in revised form, September 2, 2005
Published, MCP Papers in Press, September 9, 2005, DOI 10.1074/mcp.M500227-MCP200

[1] The abbreviations used are: GFP, green fluorescent protein; FIA, Freund's incomplete adjuvant; Ab, antibody; bis-Tris, 2-[bis(2-hydroxyethyl)amino]-2-(hydroxymethyl)propane-1,3-diol; YFP, yellow fluorescent protein; NPC, nuclear pore complex.

from the resin. The resin was then washed with a further 10 ml of lysis solution, and the wash was combined with the first elution. The sample was dialyzed against PBS, 5% glycerol and concentrated to 1 mg/ml (Centricon). This sample was submitted to Covance Immunology Services (Denver, PA) for the preparation of anti-GFP antibodies.

Anti-GFP Polyclonal Antibodies and IgG—A custom high titer anti-GFP polyclonal antibody was prepared at Covance using the in-house prepared GFP (825 μg/animal) to inject female Elite rabbits. Rabbits, selected to have no preimmune activity against the cells of interest, were injected with 250 μg of purified GFP with Freund's Complete Adjuvant (Covance). The production of antibodies was boosted and tested in the following steps: day 21, boost with 125 μg of GFP with Freund's Incomplete Adjuvant (FIA, Covance); day 31, test bleed (~5 ml of serum); day 42, boost with 125 μg of GFP with FIA; day 52, test Bleed (~5 ml of serum); day 63, boost with 125 μg of GFP with FIA; day 73, production bleed (~20 ml of serum); day 84, boost with 100 μg of GFP with FIA; day 94, production bleed (~20 ml of serum); day 105, boost with 100 μg of GFP with FIA; day 115, production bleed (~20 ml of serum); and day 118, terminal bleed (~50 ml of serum). The anti-GFP polyclonal antibodies were then affinity-purified. A CNBr-activated Sepharose 4B resin (Amersham Biosciences) was conjugated to purified GFP using the manufacturer's instructions. Purified antibody was prepared using this resin following standard antibody affinity purification procedures (17). For comparison, rabbit polyclonal antibody to GFP was also purchased from Novus Biologicals. Purified rabbit IgG was purchased from ICN Pharmaceutical.

Conjugation of Magnetic Beads—Anti-GFP polyclonal antibodies or IgG were coupled to M-270 epoxy Dynabeads (Dynal) using an optimized version of the protocol suggested by the manufacturer. Briefly, magnetic beads were washed twice with 1 ml of 0.1 M sodium phosphate buffer, pH 7.4, with a 10-min period of mixing between the washes. The beads were resuspended with anti-GFP antibodies or IgG (2.5–10 μg of Ab/1 mg of beads) followed by 0.1 M sodium phosphate buffer to bring the total volume to 13.3 μl/1 mg of beads. After gentle mixing, 6.7 μl of 3 M ammonium sulfate/1 mg of beads was added to give a total volume of ~20 μl/1 mg of beads. Conjugation was carried out overnight on a rotor at 30 °C. Saturation of 1 mg of beads was achieved with ~8 μg of antibody or IgG. Following conjugation, coupled magnetic beads were washed sequentially with 0.1 M sodium phosphate buffer, pH 7.4; 100 mM glycine-HCl, pH 2.5; 10 mM Tris, pH 8.8; freshly prepared 100 mM triethylamine solution; four washes with PBS; one 15-min wash with PBS, 0.5% Triton X-100; and one wash with PBS, and then stored at 4 °C in PBS, 0.02% NaN_3. Beads could be stored for up to 1 month after which time their efficiency for isolation decreased by ~40%.

Yeast Strains—Yeast strains expressing chromosomal fusion of the DNA fragment encoding the IgG binding domain of protein A to Kap123 and of the GFP to Kap123 and Mcm2 were a kind gift from Benjamin Timney and Vincent Archambault from the Laboratory of Cellular and Structural Biology at The Rockefeller University. Yeast strains expressing chromosomal fusion of GFP to Apl1, Nup84, Cdc14, and Arp2 were purchased from Invitrogen. Cell culture chemicals were purchased from BD Biosciences.

Plasmids and Transfections—Plasmids pEGFP-Nup37 and pEGFP-Nup43 were kindly provided by J. Cronshaw and M. Matunis (18). HeLa cells were grown in Dulbecco's modified Eagle's medium (Invitrogen) supplemented with 10% fetal calf serum, 1% L-glutamine, 100 μg/ml streptomycin, and 100 units/ml penicillin. Transfections were performed as described previously (18).

Cell Imaging—Light and fluorescence microscopy images were acquired using the DeltaVision Image Restoration microscope (Applied Precision/Olympus).

Cell Disruption and Extraction—Yeast strains were grown to ~2.0×10^7 cells/ml, harvested, and frozen as described previously (16). HeLa cells were grown to ~90% confluence, harvested in a minimal volume of PBS by gentle scraping with a rubber policeman, and frozen in liquid nitrogen. Cell lysis (both yeast and HeLa) was performed by cryogenic grinding using the Retsch MM 301 Mixer Mill (Retsch, Newtown, PA). Grinding was performed in five steps of 3min at 30 Hz inside 25-ml jars using 20-mm tungsten carbide grinding balls. The jars were cooled in liquid nitrogen between each step. An ~90% efficiency of cell disruption was confirmed by light microscopy. Lysis buffers were optimized individually for each studied protein complex (optimal conditions are given in Supplemental Table I). Lysis buffer was added to the frozen cell powder (5 ml of buffer/g of cells), and the resulting cell lysate was homogenized for 10 s with a PT 10-35 Polytron (Kinematica), then slowly rotated at 4 °C for 10–15 min, and centrifuged for 10 min at 3000 rpm at 4 °C. The resulting soluble fraction was used for the affinity purification experiments. Extraction efficiency was tested by Western blot analysis comparing the pellet and soluble fractions.

Immunoaffinity Purification—Magnetic beads, coated with anti-GFP Ab and stored at 4 °C in PBS, 0.02% NaN_3, were washed three times with lysis buffer and added to the soluble fraction of cell lysate. Immunoaffinity purifications were achieved by slow mixing at 4 °C. The magnetic beads were then collected using a Dynal magnet and washed rapidly six times with lysis buffer. The isolated protein complex was eluted from the beads for 20 min at room temperature in a fresh aqueous 0.5 N NH_4OH, 0.5 mM EDTA solution. The resulting supernatant was frozen on liquid nitrogen and left to dry overnight by vacuum centrifugation. The pellet was suspended in SDS-PAGE sample buffer, separated on a 4–12% NuPAGE Novex bis-Tris precast one-dimensional electrophoresis gel (Invitrogen) according to the manufacturer's specifications and stained with Coomassie Blue stain (Pierce) compatible with mass spectrometry.

Mass Spectrometry—Gel bands were excised into 1-mm sections, destained, washed, reduced, alkylated, and digested with 12.5 ng/μl sequencing grade modified trypsin (Promega). The resulting peptides were extracted on reverse phase resin (Poros 20 R2, PerSeptive Biosystems); eluted with 50% (v/v) methanol, 20% (v/v) acetonitrile, and 0.1% (v/v) trifluoroacetic acid; and subjected to MALDI MS analysis. An in-house built MALDI interface coupled to a quadrupole Qq-TOF instrument (QqTOF Centaur, Sciex) and an ion trap (LCQDECAXP^{PLUS}, Finnigan) were used for peptide fingerprinting (MS) and amino acid sequence analysis (MS/MS), respectively (19, 20). Computer algorithms, such as XProteo (www.xproteo.com) and PROWL (PepFrag and ProFound) (prowl.rockefeller.edu) (21), were used to correlate peptide mass fingerprint data or tandem MS CID data obtained from MS and MS/MS analyses and enabled the recognition of the proteins (22).

RESULTS

Strategy for Rapid Isolation of Protein Complexes Containing a GFP-tagged Protein—We used a single fluorescent tag to both visualize a given protein in live cells and to efficiently isolate it together with its stable interacting macromolecular partners. The method (Fig. 1) has the following sequential steps: 1) The protein of interest is tagged with GFP and visualized by fluorescence microscopy. 2) Parallel with visualization, the cells are frozen in liquid nitrogen. 3) The frozen cells are cryogenically lysed to help maintain protein complexes in their original state. 4) The GFP-tagged protein together with associated macromolecules is isolated on magnetic beads coated with polyclonal anti-GFP antibody. Isolation conditions are optimized to give efficient recovery of

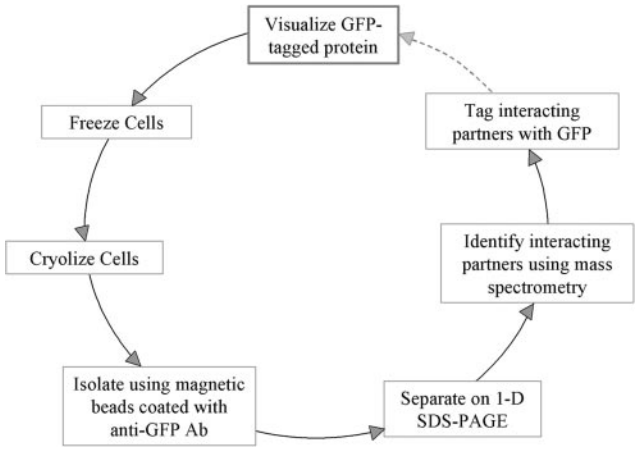

FIG. 1. **Strategy for the study of protein localization and interactions via a GFP tag.** *1-D*, one-dimensional.

the tagged protein while maintaining its native interactions. 5) The isolated proteins are eluted from the magnetic beads and resolved by one-dimensional gel electrophoresis (one-dimensional SDS-PAGE). 6) The purified proteins are identified by MALDI mass spectrometry. If desired, the identified proteins can in turn be tagged with GFP, and the cycle can be repeated. We have found this procedure to be equally efficient with cyan fluorescent protein, yellow fluorescent protein (YFP), and other variants of GFP.

To render this procedure rapid, efficient, and robust, we carefully optimized each of the steps listed above. The success of the procedure is dependent on availability of a high affinity anti-GFP antibody. Hence we raised polyclonal antisera by immunizing rabbits with a high purity full-length GFP preparation (see "Materials and Methods"); prebleeds from these rabbits had no significant nonspecific activity, and the final production bleed sera titered on Western blots to better than 1 in 10^6. Affinity-purified antibodies were prepared from these antisera using the same full-length GFP. Conjugation of the anti-GFP antibodies to magnetic beads was optimized to achieve saturation. The optimal amounts and concentrations of antibody and beads as well as the temperature and duration of the conjugation reaction are described under "Materials and Methods." Briefly saturation of 1 mg of magnetic beads was achieved with $\sim$8 μg of affinity-purified anti-GFP antibody in a total volume of 20 μl (Supplemental Fig. S1).

During the immunoisolation step, the yield of the isolated tagged protein (and any associated macromolecules) is highly dependent on the conditions used for extraction and purification. Thus, we recommend optimization of extraction and purification conditions individually for each different protein complex of interest. The efficiency of the immunoisolation on the beads is routinely $>$90%, and the recovery of this material after the high pH elution step is $>$95% (*e.g.* Fig. 2*B*). Controls with anti-GFP beads incubated in lysate from wild type yeast and yeast expressing GFP gave no significant protein signal or only GFP, respectively; similar results were obtained with wild type HeLa cells and HeLa cells expressing GFP (plus a small vimentin contaminant in the latter).

Because of the amounts needed for immunoisolations, it is preferable to generate anti-GFP antibodies in-house as described under "Materials and Methods." However, in addition to our in-house generated polyclonal anti-GFP antibody, we tested several commercially available monoclonal and polyclonal anti-GFP antibodies for their utility in protein isolation; one of these proved suitable for isolating a tagged protein but with an increased level of nonspecific binding (see "Materials and Methods" and Supplemental Fig. S2).

Visualization and Isolation of GFP-tagged Protein Complexes—We tested the applicability of this method for the analysis of numerous protein complexes located in different subcellular compartments (*e.g.* cytoplasm, nucleus, nucleolus, mitochondria, and bud neck) (Fig. 2). Hence in parallel with their *in vivo* visualization, GFP-tagged Apl1, Arp2, and Kap123 (expressed at endogenous levels) were isolated with their interacting partners from yeast whole cell extracts. Similarly GFP-tagged Nup37 and Nup43 were purified from human cell extracts. A full list of the identified interacting proteins and the conditions found optimal for these immunoaffinity purifications is given in Supplemental Table I.

AP-2R, the clathrin-associated protein complex (23), is a well characterized complex and was therefore selected as an appropriate case study for our methods (Fig. 2*A*). Apl1, the β-adaptin of the large subunit of the AP-2R complex (23), is estimated to be present at $\sim$1600 molecules per haploid cell (24). Yeast cells with GFP-tagged Apl1 expressed at endogenous levels were cultured; a small portion was examined by fluorescence microscopy, confirming the previously reported localization of Apl1 *in vivo* to the bud neck, while the rest was processed for immunopurification of Apl1-GFP with its associated macromolecular complex (Fig. 2*A*). Our method recovered Apl1-GFP in high yield (Fig. 2*B*). Protein identification by mass spectrometry confirmed the co-purification of Apl1-GFP with all the known components of the AP-2R complex: Apl3, Apm4, and Aps2 (25, 26). A schematic illustration of this complex, modified from (26), is shown in Fig. 2*A*. Additionally co-purified were Ede1 and Pmd1. Ede1 is the yeast homologue to human Eps15, which is involved in clathrin-mediated endocytosis, and was suggested to be involved in bud site selection (27, 28). Pmd1 is a low abundance protein (24) reported to be a negative regulator of sporulation (29). The MS analysis-derived expectation value and protein sequence coverage for each of the purified proteins are presented in the Supplemental Table II.

Another well characterized assembly is the Arp2/3 complex, involved in actin-based mitochondrial motility and maintenance of mitochondrial morphology, of which the actin-related protein Arp2 is a member. Our method co-purified the known members of the Arp2/3 complex (30): Arp2, Arp3, Arc35, Arc40, Arc19, Arc18, Arc15, and other associated proteins, including Ede1, Bni1, Crn1, and Actin, only some of

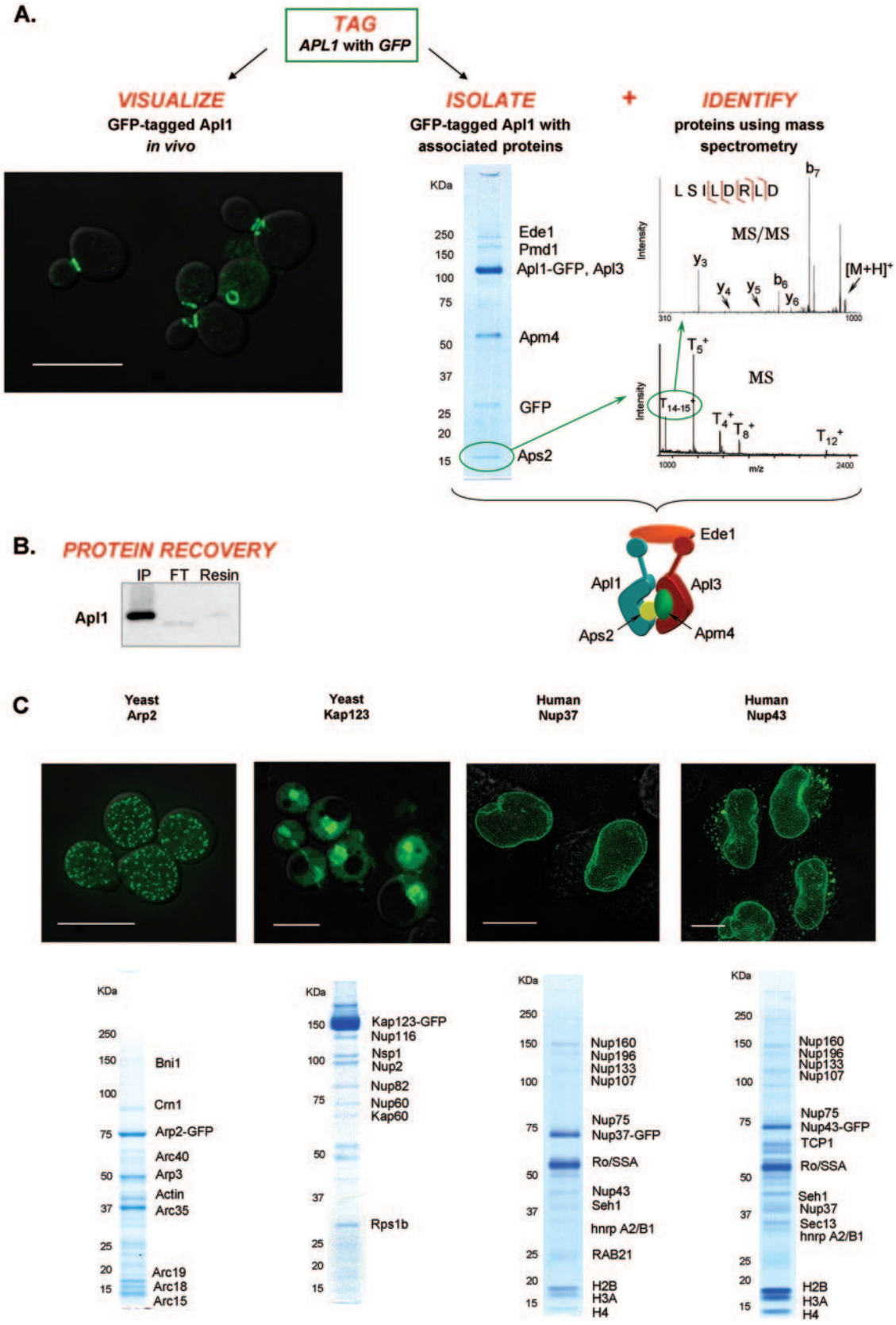
A.
TAG
APL1 with GFP
VISUALIZE
GFP-tagged Apl1
in vivo
ISOLATE
GFP-tagged Apl1 with
associated proteins
+
IDENTIFY
proteins using mass
spectrometry
KDa
250
150
100
75
50
37
25
20
15
Ede1
Pmd1
Apl1-GFP, Apl3
Apm4
GFP
Aps2
L S I L D R L D
MS/MS
Intensity
y3
y4
y5
b6
y6
b7
[M+H]+
310
1000
MS
T5+
T14-15+
T4+
T8+
T12+
1000
m/z
2400
B.
PROTEIN RECOVERY
IP
FT
Resin
Apl1
Ede1
Apl1
Apl3
Aps2
Apm4
C
Yeast
Arp2
Yeast
Kap123
Human
Nup37
Human
Nup43
KDa
250
150
100
75
50
37
25
20
15
Bni1
Crn1
Arp2-GFP
Arc40
Arp3
Actin
Arc35
Arc19
Arc18
Arc15
Kap123-GFP
Nup116
Nsp1
Nup2
Nup82
Nup60
Kap60
Rps1b
Nup160
Nup196
Nup133
Nup107
Nup75
Nup37-GFP
Ro/SSA
Nup43
Seh1
hnrp A2/B1
RAB21
H2B
H3A
H4
Nup160
Nup196
Nup133
Nup107
Nup75
Nup43-GFP
TCP1
Ro/SSA
Seh1
Nup37
Sec13
hnrp A2/B1
H2B
H3A
H4

which were previously reported to interact with Arp2 (31).

The nucleocytoplasmic transport factor Kap123 is an abundant protein involved in the import of ribosomal protein cargoes into the nucleus via the nuclear pore complex (NPC) (32), and so provides an example of a protein that interacts both with cytoplasmic proteins (its ribosomal import cargoes) and nuclear proteins (the FG repeat nucleoporins in the nuclear pore complex). As expected, the proteins that co-purified with Kap123 were indeed ribosomal protein cargo (Rps1b (32)), FG repeat nucleoporins from the nuclear pore complex (Nup60, Nsp1, Nup82, Nup116, and Nup2) (32), and Kap60, which is known to associate with Nup2 (33).

We also tested the efficacy of our anti-GFP immunopurifications in vertebrate cells. For this study, we chose two components (Nup37 and Nup43) of the human Nup107-Nup160 subcomplex, a major structural building block of the nuclear pore complex (9, 18, 34, 35). Moreover if our methods are robust and reciprocal, these two proteins should co-purify with the same set of proteins including each other; indeed this proved to be the case (Fig. 2*C*).

Effects of Incubation Time on Protein Recovery and Nonspecific Binding—During optimization of our immunoaffinity purification protocol, we observed that the length of time used for incubation of the lysate with the GFP-Ab beads had profound effects both on the efficiency and specificity of isolation of protein complexes. These effects are illustrated for the isolation of a previously well studied subcomplex from the yeast NPC, *i.e.* the Nup84 subcomplex that is known to consist of the proteins Nup133, Nup120, Nup145C, Nup85, Nup84, Seh1, and Sec13 (36–39). GFP-tagged Nup84 was isolated together with its associated proteins at a series of different incubation times (Fig. 3). At each time point, we purified all seven expected components of the Nup84 subcomplex with the amount of this subcomplex reaching a maximum after ~1 h; the major co-purifying proteins are identical to those originally reported to be present in the complex when isolated using the Protein A tag (36, 37). In addition, we observed interactions of the Nup84 complex with several other members of the NPC including the nucleoporins Nup188, Nup192, Nup157, Nup170, Pom152, Nic96, Nup145N, Nup59, Nup53, Nup57, and Nsp1 (39). Certain of these interactions (*i.e.* those between the Nup84 subcomplex and Nup157, Nup170, Nic96, and Nup145N) have been reported recently (40). Significantly the interactions that we observed between the Nup84 subcomplex and other members of the NPC were stable only at the shorter incubation times; the amount of these associated nucleoporins maximizes at ~1 h and thereafter falls off steeply with time, indicating that their interactions with the Nup84 subcomplex are weaker than those holding the components of the Nup84 subcomplex together. Another important advantage of short incubation times is in minimizing nonspecific binding as illustrated for immunopurifications of Nup84-GFP (Fig. 3) and Mcm2-GFP (47, 48) (Supplemental Fig. S3). Such nonspecific binding, typically of highly abundant proteins, is a common phenomenon in immunoisolation studies (30, 31, 41). Tests indicate that the bulk of the nonspecific binding occurs as a result of binding to the components of the affinity-purified protein complex (data not shown). In summary, the very high affinity of the anti-GFP reagent allows the use of short incubation times (≤1 h), which are advantageous both for preserving the integrity of endogenous complexes and for maximizing the amounts of the isolated complexes while minimizing the amounts of contaminants.

One concern with using short purification steps (5–30 min) is the resulting lowered yield of the tagged protein complex (Fig. 3). Therefore, we investigated the consequences of increasing amounts of anti-GFP beads during the purification, assaying both immunoisolation efficiency and nonspecific binding (Supplemental Fig. S4). The efficiency of isolation improved with the increase of resin amount up to a saturation point. The amount of resin necessary to reach saturation varies according to the amount of tagged protein in the cell lysate (*i.e.* tagged protein abundance). Nonspecific binding increased only slightly with resin amount when short incubation times were used for purification but increased significantly with longer incubation times. We conclude that short immunoisolation times and increased amounts of anti-GFP beads are optimal.

Profiling Cell Cycle-dependent Protein Complexes—Two significant challenges for any proteomic method are the study of cell state-dependent interactions and the study of interactions involving low abundance proteins. The *S. cerevisiae* phosphatase Cdc14, a key regulator of mitotic exit (42), exemplifies both challenges as it forms cell cycle-dependent interactions with proteins of low abundance. Here we en-

FIG. 2. **Visualization and isolation of GFP-tagged protein complexes.** *A*, *left*, GFP-tagged Apl1 was visualized *in vivo* in yeast cells. *Middle*, Apl1-GFP-associated proteins were immunopurified via the GFP tag, resolved by SDS-PAGE, and visualized by Coomassie Blue. Proteins were identified by mass spectrometry. *Right*, an example showing the identification of Aps2 by MALDI QqTOF MS and MALDI ion trap MS/MS analyses. T_n in the MS spectrum indicates the corresponding Aps2 residues resulting from the digestion with trypsin where *n* is the tryptic fragment number counted from the N terminus of the protein. Protein identity was confirmed by MS/MS analysis. For example, following collisionally activated dissociation, T_{14-15}^{+} underwent specific fragmentation along the peptide backbone to give rise to product ions that could be attributed to the Aps2 amino acid sequence (46). *B*, Western blot analysis of Apl1-GFP from equal fractions of the affinity-purified material (*IP*), cell lysate remaining after isolation (*FT*), and beads left after elution (*Resin*) indicate efficient isolation of the tagged protein. *C*, additional examples of the visualization and isolation of protein complexes via a GFP tag. Affinity purifications were performed on GFP-tagged Arp2, Kap123, Nup37, or Nup43 strains using 1-h incubations with conjugated magnetic beads. Eluates were resolved on SDS-PAGE and Coomassie Blue-stained. Isolated proteins were identified by mass spectrometry analysis. Specific associated proteins are labeled.

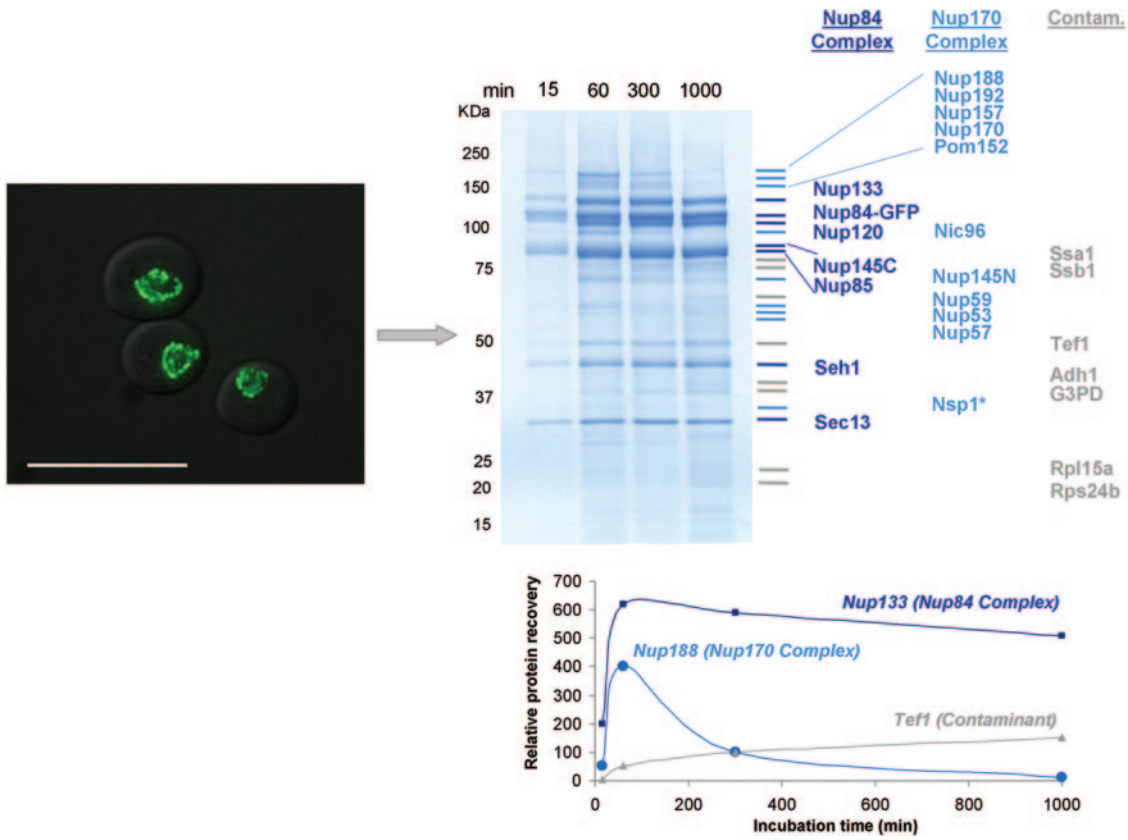

FIG. 3. **Effects of incubation times on protein recovery and nonspecific interactions.** *Left*, visualization of Nup84-GFP in yeast. *Right*, isolation of GFP-tagged Nup84 and its associated proteins using various incubation times. Proteins were identified by mass spectrometry. *Bottom*, recoveries of the indicated proteins as a function of time. *Contam.*, contaminant.

riched for interactions specific to particular cell cycle states by comparing isolations of GFP-tagged Cdc14 (expressed at endogenous levels) from 1) asynchronous cells and 2) cells arrested in the early stages of S phase using hydroxyurea (43).

Immediately prior to immunopurification, representative cells from the two populations were examined by fluorescence microscopy (Fig. 4). Upon immunopurification from asynchronous cells, GFP-tagged Cdc14 co-isolated with several proteins with which it is known to interact (including several components of the spindle pole body and known substrates of Cdc14 during mitosis (44)) as well as other proteins associated with the cell cycle that were not observed previously in immunoisolations of Cdc14 (*e.g.* Cnm67 and Cdc31) (Fig. 4*A*). Some of these proteins are present in low copy numbers in the cell, including Sli15, Nud1, Spc110, and Rad9 (24).

Following the addition of hydroxyurea, Cdc14 co-purified with most of the proteins observed in the isolates from asynchronous yeast cells (Fig. 4*B*). Notably more Net1 co-purified with the arrested cells, consistent with its role for the Net1-Cdc14 interaction in retaining Cdc14 in the nucleolus prior to mitosis (45). Additionally we observed a reduction in amount of the co-isolating spindle pole body proteins such as Nud1, Cnm67, and Cdc31.

Other proteins were found to be significantly enriched in immunopurifications from hydroxyurea-arrested cells compared with asynchronous cells; these include Sir2, Bnr1, Est1, Rad24, Ctf18, and Ctr86. Sir2 (a component of the chromatin-silencing complex) is known to interact with Cdc14; Bnr1 and Est1 are cell cycle-regulated proteins; and both Rad24 and Ctf18 are required in the cell cycle, the former as a checkpoint protein and the latter for sister chromatid cohesion. These proteins are known or suspected key players in cell cycle regulation and so are potential substrates for the Cdc14 phosphatase. Although elucidation of the functional significance of these interactions clearly requires additional experiments, our results illustrate how dynamic and rare interactions may be visualized and identified by our anti-GFP immunopurification methods.

DISCUSSION

This study reports a robust strategy that uses a single, fluorescent tag to both visualize proteins in live cells and efficiently isolate their interacting macromolecular partners. We have demonstrated the applicability of this method to the analysis of protein complexes located in various subcellular compartments and have isolated even low abundance proteins in both yeast and mammalian systems. We show that

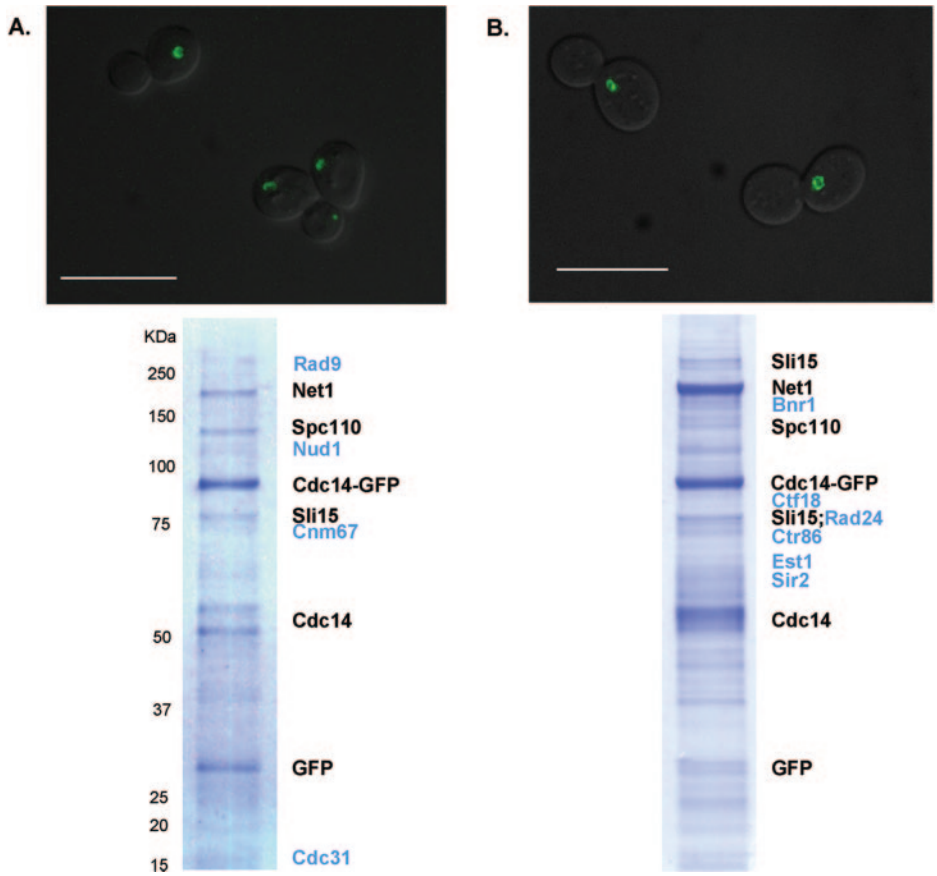

FIG. 4. **Profiling interactions specific to particular cell cycle states.** Immunoaffinity purifications of Cdc14-GFP (expressed at endogenous levels) from asynchronous cells (*A*) and cells arrested with hydroxyurea in the early stages of S phase (*B*).

high affinity anti-GFP antibodies permit rapid, single step immunoisolations, which in turn minimize nonspecific binding and maximize recovery of transiently interacting partners.

Clearly these GFP-based immunopurifications are at least as efficient as those using Protein A. However, the use of GFP as an affinity tag has significant advantages. First, the GFP tag can be both visualized and purified, allowing us to simultaneously combine information on the cellular localization of a protein with information on its interaction partners in the same cell population. Second, the expression and visualization of GFP fusion proteins does not appear to be species-dependent. Similarly our immunopurification protocol is not species-dependent as we have already immunopurified GFP-tagged proteins from viruses, bacteria, yeast, mammalian tissue culture cells, and mice. Third, there already exist a vast number of strains in which GFP has already been incorporated into a particular protein almost exclusively for the purpose of visualizing the protein within cells, tissues, or organisms. Moreover the antibody is equally efficient with cyan fluorescent protein, YFP, and other variants of GFP; by immunoblot analysis the antibody appears to have equally high titers on all these variants and has been used for immunoprecipitation of protein complexes on several variants of YFP (data not shown). Our protocol now allows the researcher to investigate the interactions made by each of the tagged proteins in all these strains. Given this wide use and availability of GFP-tagged protein reagents, the present method should greatly facilitate the elucidation of many cellular processes.

Acknowledgments—We are grateful to Alan Tackett, Svetlana Dokudovskaya, and Annick Gauthier for sharing protocols for the culture of yeast and HeLa cells, members of the Chait and Rout laboratories for useful discussions, Benjamin Timney and Vincent Archambault for the Kap123-EGFP and Mcm2-GFP strains, Michael Matunis for the EGFP-Nup37 and EGFP-Nup43 plasmids, Jonathan Rosenblum for the GFP expression plasmid, and Alison North for training on the DeltaVision microscope.

* This work was supported by National Institutes of Health Grants RR00862 (to B. T. C.), CA89810 (to B. T. C. and M. P. R.), GM062427 (to M. P. R.), RR022220 (to M. P. R. and B. T. C.), and by Women & Science fellowship Grant CEN5300379 (to I. M. C.). The costs of publication of this article were defrayed in part by the payment of page charges. This article must therefore be hereby marked "*advertisement*" in accordance with 18 U.S.C. Section 1734 solely to indicate this fact.

[S] The on-line version of this article (available at http://www.mcponline.org) contains supplemental material.

¶ To whom correspondence may be addressed: Laboratory for Mass Spectrometry and Gaseous Ion Chemistry, The Rockefeller University, 1230 York Ave., Box 170, New York, NY 10021. Tel.: 212-327-8847; Fax: 212-327-7547; E-mail: chait@mail.rockefeller.edu.

‖ To whom correspondence may be addressed: Laboratory of Cel-

lular and Structural Biology, The Rockefeller University, 1230 York Ave., Box 213, New York, NY 10021. Tel.: 212-327-8135; Fax: 212-327-7193; E-mail: rout@rockefeller.edu.

REFERENCES

1. Tsien, R. Y. (1998) The green fluorescent protein. *Annu. Rev. Biochem.* **67,** 509–544
2. Chalfie, M., Tu, Y., Euskirchen, G., Ward, W. W., and Prasher, D. C. (1994) Green fluorescent protein as a marker for gene expression. *Science* **263,** 802–805
3. van Roessel, P., and Brand, A. H. (2002) Imaging into the future: visualizing gene expression and protein interactions with fluorescent proteins. *Nat. Cell Biol.* **4,** E15–E20
4. Huh, W. K., Falvo, J. V., Gerke, L. C., Carroll, A. S., Howson, R. W., Weissman, J. S., and O'Shea, E. K. (2003) Global analysis of protein localization in budding yeast. *Nature* **425,** 686–691
5. Dziembowski, A., and Seraphin, B. (2004) Recent developments in the analysis of protein complexes. *FEBS Lett.* **556,** 1–6
6. Kellogg, D. R., and Moazed, D. (2002) Protein and immunoaffinity purification of multiprotein complexes. *Methods Enzymol.* **351,** 172–183
7. Einhauer, A., and Jungbauer, A. (2001) The FLAG peptide, a versatile fusion tag for the purification of recombinant proteins. *J. Biochem. Biophys. Methods* **49,** 455–465
8. Puig, O., Caspary, F., Rigaut, G., Rutz, B., Bouveret, E., Bragado-Nilsson, E., Wilm, M., and Seraphin, B. (2001) The tandem affinity purification (TAP) method: a general procedure of protein complex purification. *Methods* **24,** 218–229
9. Loiodice, I., Alves, A., Rabut, G., Van Overbeek, M., Ellenberg, J., Sibarita, J. B., and Doye, V. (2004) The entire Nup107-160 complex, including three new members, is targeted as one entity to kinetochores in mitosis. *Mol. Biol. Cell* **15,** 3333–3344
10. Hu, X., Wang, L., Lu, P., Chilvers, M. M., and Gao, X. (1999) Expression and analysis of recombinant human IL-18 and human IL-18-GFP fusion protein. *Zhonghua Weishengwuxue He Mianyixue Zazhi* **19,** 306–310
11. Obuse, C., Iwasaki, O., Kiyomitsu, T., Goshima, G., Toyoda, Y., and Yanagida, M. (2004) A conserved Mis12 centromere complex is linked to heterochromatic HP1 and outer kinetochore protein Zwint-1. *Nat. Cell Biol.* **6,** 1135–1141
12. Iijima, M., Huang, Y. E., Luo, H. R., Vazquez, F., and Devreotes, P. N. (2004) Novel mechanism of PTEN regulation by its phosphatidylinositol 4,5-bisphosphate binding motif is critical for chemotaxis. *J. Biol. Chem.* **279,** 16606–16613
13. Cheeseman, I. M., Niessen, S., Anderson, S., Hyndman, F., Yates, J. R., III, Oegema, K., and Desai, A. (2004) A conserved protein network controls assembly of the outer kinetochore and its ability to sustain tension. *Genes Dev.* **18,** 2255–2268
14. Kops, G. J., Kim, Y., Weaver, B. A., Mao, Y., McLeod, I., Yates, J. R., III, Tagaya, M., and Cleveland, D. W. (2005) ZW10 links mitotic checkpoint signaling to the structural kinetochore. *J. Cell Biol.* **169,** 49–60
15. Cheeseman, I. M., MacLeod, I., Yates, J. R., III, Oegema, K., and Desai, A. (2005) The CENP-F-like proteins HCP-1 and HCP-2 target CLASP to kinetochores to mediate chromosome segregation. *Curr. Biol.* **15,** 771–777
16. Archambault, V., Li, C. X., Tackett, A. J., Wasch, R., Chait, B. T., Rout, M. P., and Cross, F. R. (2003) Genetic and biochemical evaluation of the importance of Cdc6 in regulating mitotic exit. *Mol. Biol. Cell* **14,** 4592–4604
17. Harlow, E., and Lane, D. (1988) in *Antibodies: A laboratory Manual*, pp. 314–315, Cold Spring Harbor Laboratory, Cold Spring Harbor, NY
18. Cronshaw, J. M., Krutchinsky, A. N., Zhang, W., Chait, B. T., and Matunis, M. J. (2002) Proteomic analysis of the mammalian nuclear pore complex. *J. Cell Biol.* **158,** 915–927
19. Krutchinsky, A. N., Zhang, W., and Chait, B. T. (2000) Rapidly switchable matrix-assisted laser desorption/ionization and electrospray quadrupole-time-of-flight mass spectrometry for protein identification. *J. Am. Soc. Mass Spectrom.* **11,** 493–504
20. Krutchinsky, A. N., Kalkum, M., and Chait, B. T. (2001) Automatic identification of proteins with a MALDI-quadrupole ion trap mass spectrometer. *Anal. Chem.* **73,** 5066–5077
21. Zhang, W., and Chait, B. T. (2000) ProFound: an expert system for protein identification using mass spectrometric peptide mapping information. *Anal. Chem.* **72,** 2482–2489
22. Cristea, I. M., Gaskell, S. J., and Whetton, A. D. (2004) Proteomics techniques and their application to hematology. *Blood* **103,** 3624–3634
23. Yeung, B. G., Phan, H. L., and Payne, G. S. (1999) Adaptor complex-independent clathrin function in yeast. *Mol. Biol. Cell* **10,** 3643–3659
24. Ghaemmaghami, S., Huh, W. K., Bower, K., Howson, R. W., Belle, A., Dephoure, N., O'Shea, E. K., and Weissman, J. S. (2003) Global analysis of protein expression in yeast. *Nature* **425,** 737–741
25. Boehm, M., and Bonifacino, J. S. (2001) Adaptins: the final recount. *Mol. Biol. Cell* **12,** 2907–2920
26. Boehm, M., and Bonifacino, J. S. (2002) Genetic analyses of adaptin function from yeast to mammals. *Gene* (*Amst.*) **286,** 175–186
27. Gagny, B., Wiederkehr, A., Dumoulin, P., Winsor, B., Riezman, H., and Haguenauer-Tsapis, R. (2000) A novel EH domain protein of Saccharomyces cerevisiae, Ede1p, involved in endocytosis. *J. Cell Sci.* **113,** 3309–3319
28. Ni, L., and Snyder, M. (2001) A genomic study of the bipolar bud site selection pattern in Saccharomyces cerevisiae. *Mol. Biol. Cell* **12,** 2147–2170
29. Benni, M. L., and Neigeborn, L. (1997) Identification of a new class of negative regulators affecting sporulation-specific gene expression in yeast. *Genetics* **147,** 1351–1366
30. Aloy, P., Bottcher, B., Ceulemans, H., Leutwein, C., Mellwig, C., Fischer, S., Gavin, A. C., Bork, P., Superti-Furga, G., Serrano, L., and Russell, R. B. (2004) Structure-based assembly of protein complexes in yeast. *Science* **303,** 2026–2029
31. Ho, Y., Gruhler, A., Heilbut, A., Bader, G. D., Moore, L., Adams, S. L., Millar, A., Taylor, P., Bennett, K., Boutilier, K., Yang, L., Wolting, C., Donaldson, I., Schandorff, S., Shewnarane, J., Vo, M., Taggart, J., Goudreault, M., Muskat, B., Alfarano, C., Dewar, D., Lin, Z., Michalickova, K., Willems, A. R., Sassi, H., Nielsen, P. A., Rasmussen, K. J., Andersen, J. R., Johansen, L. E., Hansen, L. H., Jespersen, H., Podtelejnikov, A., Nielsen, E., Crawford, J., Poulsen, V., Sorensen, B. D., Matthiesen, J., Hendrickson, R. C., Gleeson, F., Pawson, T., Moran, M. F., Durocher, D., Mann, M., Hogue, C. W., Figeys, D., and Tyers, M. (2002) Systematic identification of protein complexes in Saccharomyces cerevisiae by mass spectrometry. *Nature* **415,** 180–183
32. Rout, M. P., Blobel, G., and Aitchison, J. D. (1997) A distinct nuclear import pathway used by ribosomal proteins. *Cell* **89,** 715–725
33. Dilworth, D. J., Suprapto, A., Padovan, J. C., Chait, B. T., Wozniak, R. W., Rout, M. P., and Aitchison, J. D. (2001) Nup2p dynamically associates with the distal regions of the yeast nuclear pore complex. *J. Cell Biol.* **153,** 1465–1478
34. Walther, T. C., Alves, A., Pickersgill, H., Loiodice, I., Hetzer, M., Galy, V., Hulsmann, B. B., Kocher, T., Wilm, M., Allen, T., Mattaj, I. W., and Doye, V. (2003) The conserved Nup107-160 complex is critical for nuclear pore complex assembly. *Cell* **113,** 195–206
35. Grandi, P., Dang, T., Pane, N., Shevchenko, A., Mann, M., Forbes, D., and Hurt, E. (1997) Nup93, a vertebrate homologue of yeast Nic96p, forms a complex with a novel 205-kDa protein and is required for correct nuclear pore assembly. *Mol. Biol. Cell* **8,** 2017–2038
36. Siniossoglou, S., Wimmer, C., Rieger, M., Doye, V., Tekotte, H., Weise, C., Emig, S., Segref, A., and Hurt, E. C. (1996) A novel complex of nucleoporins, which includes Sec13p and a Sec13p homolog, is essential for normal nuclear pores. *Cell* **84,** 265–275
37. Siniossoglou, S., Lutzmann, M., Santos-Rosa, H., Leonard, K., Mueller, S., Aebi, U., and Hurt, E. (2000) Structure and assembly of the Nup84p complex. *J. Cell Biol.* **149,** 41–54
38. Lutzmann, M., Kunze, R., Buerer, A., Aebi, U., and Hurt, E. (2002) Modular self-assembly of a Y-shaped multiprotein complex from seven nucleoporins. *EMBO J.* **21,** 387–397
39. Rout, M. P., Aitchison, J. D., Suprapto, A., Hjertaas, K., Zhao, Y., and Chait, B. T. (2000) The yeast nuclear pore complex: composition, architecture, and transport mechanism. *J. Cell Biol.* **148,** 635–651
40. Lutzmann, M., Kunze, R., Stangl, K., Stelter, P., Toth, K. F., Bottcher, B., and Hurt, E. (2005) Reconstitution of Nup157 and Nup145N into the Nup84 complex. *J. Biol. Chem.* **280,** 18442–18451
41. Archambault, V., Chang, E. J., Drapkin, B. J., Cross, F. R., Chait, B. T., and Rout, M. P. (2004) Targeted proteomic study of the cyclin-Cdk module. *Mol. Cell* **14,** 699–711
42. Stegmeier, F., and Amon, A. (2004) Closing mitosis: the functions of the

Cdc14 phosphatase and its regulation. *Annu. Rev. Genet.* **38,** 203–232
43. Wan, J., Xu, H., and Grunstein, M. (1992) CDC14 of *Saccharomyces cerevisiae*. Cloning, sequence analysis, and transcription during the cell cycle. *J. Biol. Chem.* **267,** 11274–11280
44. Muller, E. G., Snydsman, B. E., Novik, I., Hailey, D. W., Gestaut, D. R., Niemann, C. A., O'Toole, E. T., Giddings, T. H., Jr., Sundin, B. A., and Davis, T. N. (2005) The organization of the core proteins of the yeast spindle pole body. *Mol. Biol. Cell* **16,** 3341–3352f
45. Shou, W., Seol, J. H., Shevchenko, A., Baskerville, C., Moazed, D., Chen, Z. W., Jang, J., Charbonneau, H., and Deshaies, R. J. (1999) Exit from mitosis is triggered by Tem1-dependent release of the protein phosphatase Cdc14 from nucleolar RENT complex. *Cell* **97,** 233–244
46. Qin, J., and Chait, B. T. (1996) Matrix-assisted laser desorption ion trap mass spectrometry: efficient isolation and effective fragmentation of peptide ions. *Anal. Chem.* **68,** 2108–2112
47. Davey, M. J., Indiani, C., and O'Donnell, M. (2003) Reconstitution of the Mcm2-7p heterohexamer, subunit arrangement, and ATP site architecture. *J. Biol. Chem.* **278,** 4491–4499
48. Tanaka, S., and Diffley, J. F. (2002) Interdependent nuclear accumulation of budding yeast Cdt1 and Mcm2-7 during G1 phase. *Nat. Cell. Biol.* **4,** 198–207
49. Flory, M. R., Carson, A. R., Muller, E. G., and Aebersold, R. (2004) An SMC-domain protein in fission yeast links telomeres to the meiotic centrosome. *Mol. Cell.* **16,** 619–630